How colors influence numbers: Photon statistics of parametric down-conversion

Wolfgang Mauerer,* Malte Avenhaus, Wolfram Helwig, and Christine Silberhorn

Max Planck Research Group, Institute of Optics, Information and Photonics, Junior Research Group IQO,
Günther-Scharowsky-Straße 1/Bau 24, 91058 Erlangen, Germany

Parametric down-conversion (PDC) is a technique of ubiquitous experimental significance in the production of nonclassical, photon-number-correlated twin beams. Standard theory of PDC as a two-mode squeezing process predicts and homodyne measurements observe a thermal photon number distribution per beam. Recent experiments have obtained conflicting distributions. In this article, we explain the observation by an *a priori* theoretical model solely based on directly accessible physical quantities. We compare our predictions with experimental data and find excellent agreement.

I. INTRODUCTION

The quantum characteristics of free-propagating light pulses generated by $\chi^{(2)}$ nonlinearities are traditionally studied using homodyne detection. Unfortunately, this standard technique implicitly restricts the observation to an effective single spectral mode imposed by the single local oscillator. Detectors based on avalanche photodiodes [1], in contrast, are sensitive on all modes generated by sources of current experimental significance and uncover richer spectral properties. This substructure is currently usually neglected or only treated effectively, although it impacts security proofs of quantum key distribution [2] or the validity of the conditional preparation of pulsed non-Gaussian states [3].

Recent experiments have observed that the photon number distribution (PND) for multimode sources differs markedly from the prediction of the single-mode standard model [4]. In this article, we show that the PND is a direct consequence of the internal spectral structure of PDC states. By establishing an *a priori* theoretical explanation, we demonstrate the intrinsic connection between the spectral correlations of signal and idler mode and the observed PND.

Our approach explains this behavior by decomposing the state into a set of independent two-mode squeezers [5,6]: from the complex spectral structure composed of a mode continuum, we derive a significantly smaller number of fundamental contributions that nevertheless fully capture the physics of the source. The properties of the individual contributions are well known and allow us to infer the properties of the complete system.

In contrast to previous efforts (for instance [7,8], but observe also the references therein), our approach enables the quantitative computation of photon number statistics *without* assumptions or fitting of nonphysical parameters. This is important for a wide class of experiments ranging from fundamental to highly applied because they require a complete understanding of the internal structure of PDC states to fully exploit their quantum features.

II. DECOMPOSITION

A multimode type-II down-conversion process is most conveniently studied using the interaction Hamiltonian

$\hat{H}_{\mathrm{int}}(t) = \int_V d^3\vec{x} \chi^{(2)} \hat{E}_p^{(+)}(\vec{x},t)\hat{E}_s^{(-)}(\vec{x},t)\hat{E}_i^{(-)}(\vec{x},t) + \mathrm{H.c.}$ [9], where the subscripts denote pump, signal, and idler, respectively, and the tensor $\chi^{(2)}$ represents the second-order nonlinear susceptibility. By assuming a classical pump and a frequency-independent $\chi^{(2)}$ in the spectral range of interest, it can be shown [10] that with $\hat{H}_I \equiv \int_{t_0}^t dt' \hat{H}_{\mathrm{int}}(t')$,

$$\hat{H}_I = C \int \int d\omega_1 d\omega_2 f(\omega_1,\omega_2)\hat{a}^\dagger(\omega_1)\hat{b}^\dagger(\omega_2) + \mathrm{H.c.}, \quad (1)$$

where $\hat{a}^\dagger(\omega_1)$ and $\hat{b}^\dagger(\omega_2)$ are field operators that create a monochromatic photon with frequency ω_i in the signal and idler modes a and b. $f(\omega_1,\omega_2)$ is the spectral distribution function (SDF) of the single photon contribution and $C = C(\chi^{(2)}, \sqrt{I_p})$ is a coupling constant that depends on the strength $\chi^{(2)}$ of the nonlinear susceptibility and on the pump intensity [9,11]. The time-propagated state is computed by $|\psi\rangle = \mathcal{T}\exp[(i\hbar)^{-1}\hat{H}_I]|\psi(t_0)\rangle$, where we assume that the pulse has completely left the crystal and the interaction is finished. Following [10], the time ordering $\mathcal{T}$ can be omitted because the Hamiltonian approximately commutes with itself at different times and the corrections are therefore negligible.

To express $\hat{H}_I$ in a more convenient form, we use the Schmidt decomposition of $f(\omega_1,\omega_2)$, uniquely defined by

$$f(\omega_1,\omega_2) = \sum_{n=0}^{N-1} \sqrt{\lambda_n}\,\xi_n^{(1)}(\omega_1)\xi_n^{(2)}(\omega_2), \quad (2)$$

where the Schmidt modes $\{\xi_n^{(1)}(\omega_1)\}$ and $\{\xi_n^{(2)}(\omega_2)\}$ are two sets of orthonormal bases with respect to the L^2 inner product, and the Schmidt eigenvalues λ_n are real expansion coefficients that satisfy $\Sigma_n \lambda_n = 1$. The salient feature of Eq. (2) is that only a single summation index is required and not two as for a regular change of basis. The decomposition is guaranteed to exist for a large class of systems under very general assumptions [12]. For simple systems that require only a few Schmidt modes (i.e., N is small), the decomposition can be numerically computed by solving a set of coupled integral equations [13]. For systems that require a large N, it is usually easier to perform a singular value decomposition (SVD); see Ref. [14] and below for more details.

*wm@linux-kernel.net

We define effective single-mode field operators (sometimes also called pseudoboson operators) by

$$\hat{A}_n^\dagger \equiv \int d\omega \, \xi_n^{(1)}(\omega) \hat{a}^\dagger(\omega), \tag{3}$$

and similarly for $\hat{B}_n$. Because the spectral distribution functions are orthonormal, that is, $\langle \xi_i, \xi_j \rangle = \delta_{ij}$, it is easy to verify that the operators fulfill the canonical commutation relations $[\hat{A}_j, \hat{A}_k^\dagger] = \hat{1}\delta_{jk}$ and $[\hat{A}_j, \hat{A}_k] = 0$. More details about this notation are provided by Ref. [15].

By rewriting $\hat{H}_I$ in Eq. (1) using Schmidt decomposition (2) for $f(\omega_1, \omega_2)$ and the definition of pseudoboson operators in Eq. (3), we obtain

$$\exp\left(\frac{1}{i\hbar}\hat{H}_I\right) = \exp\left(\frac{C}{i\hbar}\sum_{n=0}^{N-1}\sqrt{\lambda_n}\hat{A}_n^\dagger\hat{B}_n^\dagger + \text{H.c.}\right). \tag{4}$$

The two-mode squeezing operator for spectral effective single modes A, B is defined by $\hat{S}_{AB}(\eta_n) \equiv \exp(-\eta_n\hat{A}^\dagger\hat{B}^\dagger + \eta_n^*\hat{A}\hat{B})$, where $\eta_n = C\sqrt{\lambda_n}/(i\hbar) \equiv r_n \exp i\varphi_n$ is a complex number. Because $[\hat{A}_j, \hat{A}_k^\dagger] = 0$ for $j \neq k$, the state after the interaction is a tensor product of independent two-mode squeezers [16]:

$$|\psi\rangle = \overset{N-1}{\underset{n=0}{\otimes}} \hat{S}_{A_nB_n}(\eta_n)|\psi(t_0)\rangle. \tag{5}$$

This decomposition allows us to inspect the SDF using a small number of elementary contributions whose properties are well known and avoids the need to consider the complicated raw correlations. Another consequence of Eq. (5) is that the SDF is identical for all orders of photon number contributions because creation operators that belong to different distribution functions are never mixed [17].

III. COMPUTING STATISTICAL DISTRIBUTIONS

For two-mode squeezed states, the PND in each mode is thermal, that is, for the state

$$|\psi\rangle = \hat{S}_{AB}(\eta)|00\rangle = \sum_{n=0}^{\infty}\kappa_n|n,n\rangle, \tag{6}$$

the distribution is given by $p(n) = |\kappa_n|^2 = \text{sech}^2 r \tanh^{2n} r$ for one output mode, that is, $N = 1$. Consequently, the photon number distribution of multimode state (5) is given by the convolution of the distributions of all independent squeezers. Assume that $p_{\xi_k}(n)$ denotes the PND of the kth squeezer with spectral modes $\xi_k^{(i)}$. The overall PND is then given by

$$p_{\vec{\xi}}(n) = \sum_{\Theta \in n \vdash N}\prod_{m=0}^{N-1}p_{\xi_m}(\Theta_m), \tag{7}$$

where $n \vdash N$ denotes the set of all partitions of n into N parts. The distribution $p_{\vec{\xi}}(n)$ is consequently the convolution of all probability distributions $p_{\xi_i}(n)$.

Two special cases follow directly from Eq. (7): when only a single effective mode contributes ($N = 1$), the resulting dis-

tribution exhibits thermal behavior. When the physical process requires a very large number of effective modes ($N \to \infty$), the resulting PND is Poissonian, because it is known that a convolution of thermal distributions converges to a Poissonian distribution in this limit [18].

Computing the convolution in Eq. (7) involves summing over numerous contributions. This is considerably simplified by using generating functions. For coefficients $p(n)$, they are given by the formal power series [18] $g(\zeta) = \sum_n p(n)\zeta^n$. The individual coefficients can be recovered via $p(n) = (1/n!)(\partial^n/\partial x^n) g(\zeta)|_{\zeta=0}$. For the thermal distribution of a two-mode squeezer, the series converges analytically to $g_k(\zeta) = \text{sech}^2 r_k/1 - \zeta \tanh^2 r_k$, where r_k is the strength of the kth squeezer. The generating function for a convolution of N thermal distributions is $\prod_{k=0}^{N-1}g_k(\zeta)$ and the resulting photon number distribution is consequently

$$p_{\vec{\xi}}(n) = \frac{1}{n!}\left[\frac{\partial^n}{\partial\zeta^n}\prod_{k=0}^{N-1}g_k(\zeta)\right]\Bigg|_{\zeta=0}. \tag{8}$$

This representation allows us to compute the statistical distribution composed of many contributions with modest computational effort.

Let us now turn our attention to an example illustrating our considerations. Assume that the SDF is given by a two-dimensional, real-valued Gaussian distribution (this is not a restriction because the methods also work for complex, non-Gaussian SDFs). This approximation is commonly used [13,19] to provide a convenient parametrization of type-II PDC processes. Especially, it is possible to perform an analytical Schmidt decomposition (a similar approach is used, for instance, in Ref. [19]). We use the parameters σ_x^2 and σ_y^2 to specify the spectral widths of signal and idler, while θ denotes the rotation with respect to the x axis. This form is illustrated in Fig. 3.

Let us choose $\sigma_x^2 = 25$ and $\sigma_y^2 = 1$, which are the parameters depicted in the inset of Fig. 3. The Schmidt number $K = 1/\Sigma_n\lambda_n^2$ is computed from the eigenvalues λ_n of the Schmidt decomposition. It is a measure for the number of effectively contributing spectral modes and thus of inherent spectral correlations of the physical process [13] (notice that we could have also considered an entanglement monotone like the logarithmic negativity for this purpose). For $\theta = 0$, the state exhibits no spectral correlations and a single Schmidt mode suffices for the decomposition. By rotating the SDF from $\theta = 0$ to $\theta = \pi/2$, the correlations increase to their maximal value at $\theta = \pi/4$ and decrease again until the SDF becomes separable for $\theta = \pi/2$. This implies thermal statistics for $\theta = 0$ and $\theta = \pi/2$ and maximal similarity to Poissonian statistics for $\theta = \pi/4$. The coupling and pump intensity are, for better comparability, chosen such that $\bar{n} = 1$ for all PNDs. Figure 1 illustrates the arising distributions.

To quantify the difference between convoluted and Poissonian or thermal distributions, we employ the variational distance defined for two probability distributions p_1 and p_2 as $\Delta_{p_1,p_2} \equiv \Sigma_n|p_1(n) - p_2(n)|$. Two distributions are completely identical if and only if $\Delta = 0$. Figure 2 compares the difference of the convoluted distribution to the above-mentioned special cases for a growing Schmidt number K, that is, a
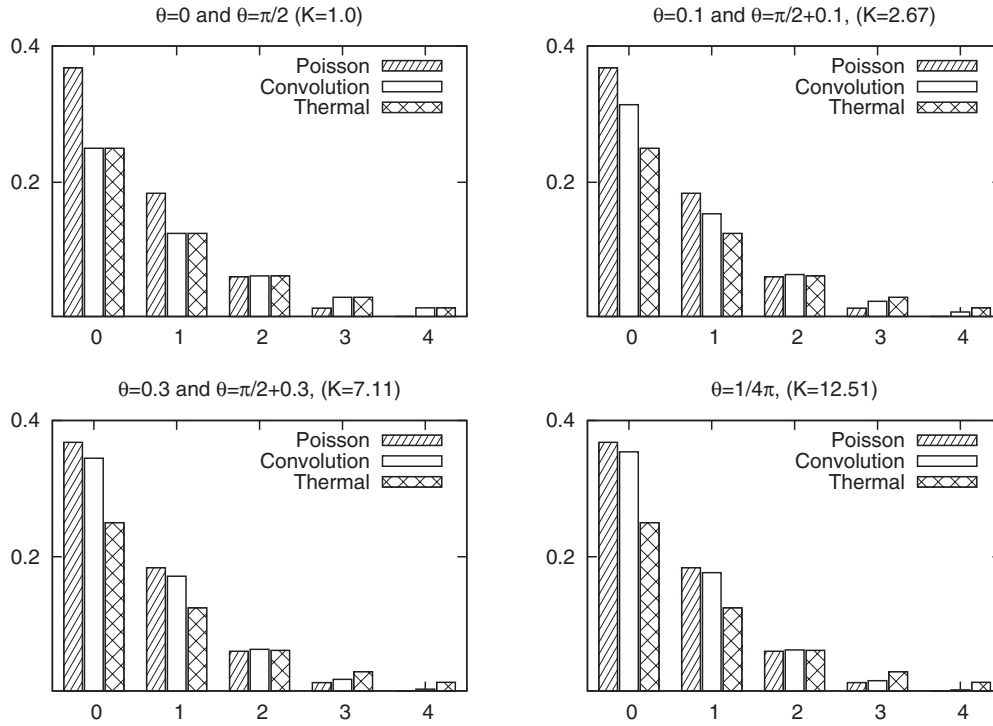
FIG. 1. Photon number distribution depending on the number of effectively contributing modes as given by the Schmidt number K (and thus on the angle of the SDF) of a type-II PDC process. The x axes depict photon numbers, whereas the y axes show probabilities.

growing number of Schmidt modes achieved by rotating the Gaussian SDF for $\theta=0$ to $\theta=\pi/4$. Once again, we emphasize that the shift toward a Poissonian distribution is inherent in the physical process and not caused by any experimental imperfections.

IV. COMPARISON WITH EXPERIMENTAL DATA

We have also performed a comparison of experimentally measured photon number statistics with the predictions of

our theory. A photon-number-resolving fiber-loop detector [1] in combination with highly efficient waveguides was used to record the distribution. The detection method is resilient against loss and allows us to eliminate the corresponding effects when ensemble measurements are performed. Reference [20] shows the experimental details of state generation and [4] describes the measurement procedure. Figure 3 compares the experimentally observed distribution with the theoretical prediction at various pump powers. As is imme-
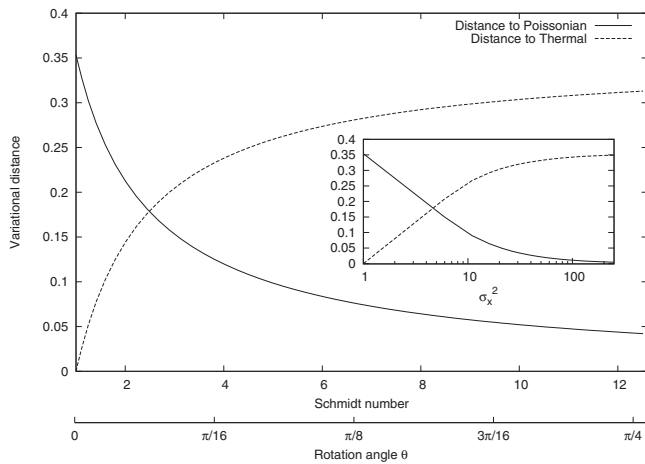

FIG. 2. Solid line and dashed line show the distance between the convoluted photon number distribution and Poissonian or thermal statistics, respectively, plotted against the Schmidt number. For a single effective mode, the distribution is exactly thermal, but the more modes contribute, the closer it gets to a Poissonian distribution. The inset fixes $\theta=\pi/4$ and varies σ_x^2, which is drawn on a logarithmic scale.
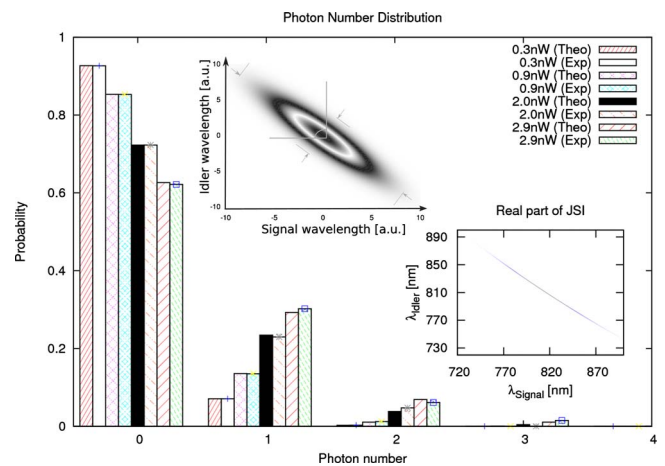

FIG. 3. (Color online) Comparison between experimentally measured and theoretically obtained photon number distributions for a multimode PDC process at various pump strengths. The bottom inset shows the real part of the joint spectral intensity, while the top inset demonstrates the parametrization of the analytical Gaussian approximation of the SDF. Loss inversion and error estimation was performed using non-negative least-squares optimization.
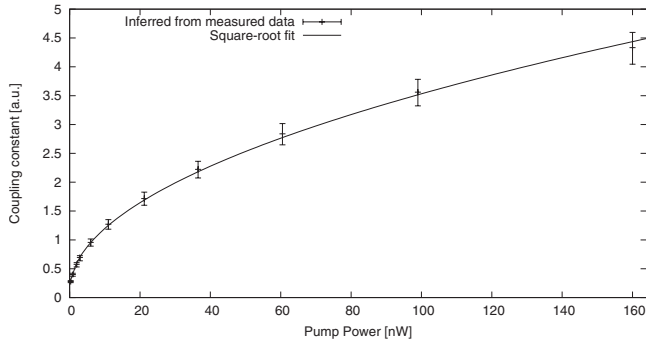
FIG. 4. Relation between pump power and coupling parameter. The expected square-root dependency [11] is correctly obtained for a wider range of pump intensities than can be resolved with current TMDs, which ensures the validity of our approach also for high powers. Notice that this knowledge would also allow for computing the expected mean photon number for a given pump power or a determination of $\chi^{(2)}$, as described in [23].

diately obvious from the figure, they are in excellent agreement.

To avoid the necessity of fitting any effective parameters, we have obtained an exact numerical decomposition using SVD techniques. After discretizing the SDF on a grid M_{mn} of size 1500×1500, the matrix is decomposed as $M = U\Sigma V^{\dagger}$, where U and V are unitaries and $\Sigma = \text{diag}(\sqrt{\lambda_1}, \ldots, \sqrt{\lambda_N})$ is a real diagonal matrix [21]. Extensive checks that the decomposition converges (and also converges to the proper value) have been performed; see Ref. [14] for details.

Notice that the decomposition of the spectral distribution does *not* depend on the pump intensity, which means that the composition $\{\lambda_n\}$ of the PND is fixed for the physical process. However, the observed *mean value* of the PND does depend on the pump intensity and Fig. 3 shows a shift toward larger mean photon numbers for larger pump intensities as expected.

For higher pump powers, photon-number-resolved detection is not possible anymore. To check the theory in this regime, we have used a set of mean photon number ($\bar{n}$) measurements instead. The coupling constant C as defined in Eq. (1) can be inferred from the decomposed SDF for each $\bar{n}$ for a given pump power by a numerical optimization process

[22]. The result is shown in Fig. 4. Again, very good agreement between theory and experiment is achieved.

V. CONCLUSIONS

We have shown how to decompose a multimode PDC process into independent two-mode squeezers operating on effective single modes and how this explains why the photon number distribution of the process can exhibit any form ranging from purely thermal to purely Poissonian. We have underlined the validity of the theory by comparing the predictions to an experimentally measured photon number distribution. Additionally, we have compared theory and experiment for larger pump powers.

APPENDIX

A two-dimensional Gaussian distribution in a suitable parametrization is given by

$$f(x,y) = \frac{1}{\sqrt{\pi}\sigma_x\sigma_y}\exp(-ax^2 - 2bxy - cy^2),$$

$$a(\theta, \sigma_x, \sigma_y) = \cos^2\theta/(2\sigma_x^2) + \sin^2\theta/(2\sigma_y^2),$$

$$b(\theta, \sigma_x, \sigma_y) = -\sin 2\theta/(4\sigma_x^2) + \sin 2\theta/(4\sigma_y^2),$$

$$c(\theta, \sigma_x, \sigma_y) = \sin^2\theta/(2\sigma_x^2) + \cos^2\theta/(2\sigma_y^2).$$

Without getting into details of the algebra involved, we remark that by starting from Mehler's formula [24] $\sum_{n=0}^{\infty} H_n(x)H_n(y)(\frac{1}{2}\gamma)^n/n! = 1/\sqrt{1-\gamma^2}\exp(-\gamma^2 x^2 - 2\gamma xy + \gamma^2 y^2/1-\gamma^1)$ [$H_n(x)$ denotes the Hermite polynomial of nth order], it is possible to bring $f(x,y)$ into the form $f(x,y) = \sum_{n=0}^{\infty}\sqrt{\lambda_n}f_n^{(1)}(x)f_n^{(2)}(y)$. The coefficients λ_n are given by $\lambda_n = (2^{2n-1}/ac)(1+\gamma^2/\sigma_x\sigma_y)(\gamma/2)^{2n}$ where $\gamma = -2\sqrt{ac} + \sqrt{4ac - 4b^2}/2b$. Since the set $\{\lambda_n\}$ contains all information required for our calculations, the exact form of $f_n^{(i)}(\cdot)$ is not of interest here, but can be found in Ref. [23].

[1] D. Achilles, C. Silberhorn, C. Sliwa, K. Banaszek, and I. A. Walmsley, Opt. Lett. **28**, 2387 (2003).

[2] W. Helwig, Master's thesis, FAU Erlangen-Nürnberg, 2008.

[3] A. Ourjoumtsev, H. Jeong, R. Tualle-Brouri, and P. Grangier, Nature (London) **448**, 784 (2007).

[4] M. Avenhaus, H. B. Coldenstrodt-Ronge, K. Laiho, W. Mauerer, I. A. Walmsley, and C. Silberhorn, Phys. Rev. Lett. **101**, 053601 (2008).

[5] S. L. Braunstein, Phys. Rev. A **71**, 055801 (2005).

[6] W. Wasilewski, A. I. Lvovsky, K. Banaszek, and C. Radzewicz, Phys. Rev. A **73**, 063819 (2006).

[7] J. Perina, Jr., O. Haderka, and M. Hamar, e-print arXiv:quant-ph/0310065.

[8] W. Wasilewski, C. Radzewicz, R. Frankowski, and K. Banaszek, Phys. Rev. A **78**, 033831 (2008).

[9] F. Dell'Anno, S. De Siena, and F. Illuminati, Phys. Rep. **428**, 53 (2006).

[10] W. P. Grice and I. A. Walmsley, Phys. Rev. A **56**, 1627 (1997).

[11] M. I. Kolobov, Rev. Mod. Phys. **71**, 1539 (1999).

[12] S. Parker, S. Bose, and M. B. Plenio, Phys. Rev. A **61**, 032305 (2000).

[13] C. K. Law, I. A. Walmsley, and J. H. Eberly, Phys. Rev. Lett. **84**, 5304 (2000).

[14] W. Mauerer and C. Silberhorn, *Numerical Analysis of Parametric Downconversion*, Proceeding of the Eighth International Conference on Quantum Communication, Measurement, and Computing, Calgary, Canada (2008).

[15] P. P. Rohde, W. Mauerer, and C. Silberhorn, New J. Phys. **9**, 91 (2007).

[16] By recoupling (neglecting unimportant phases) $\hat{A}_j \rightarrow 1/\sqrt{2}(\hat{C}_j - \hat{D}_j)$, $\hat{B}_j \rightarrow 1/\sqrt{2}(\hat{D}_j + \hat{C}_j)$, it follows that $\hat{S}_{A_j B_j}(\eta) = \hat{S}_{C_j}(\eta) \otimes \hat{S}_{D_j}(\eta)$, that is, a product of two independent effective single-mode squeezers [25]. Using this transformation, we obtain the standard Bloch-Messiah decomposition (see, e.g., Refs. [5,6]). Owing to the coupling of the signal mode A_j with the idler mode B_j, this form delivers the joint photon number distribution for signal and idler, $p_{\text{joint}}(n)$. It is connected to our distribution via $p_{\text{joint}}(2n) = p(n)$, and $p_{\text{joint}}(2n+1) = 0$. When a degenerate PDC process (including type I) with $\hat{A}_j = \hat{B}_j$ is considered, the decomposition in Eq. (4) automatically leads to the Bloch-Messiah decomposition.

[17] This property can already be inferred from Eq. (4) by defining the operators $\hat{K}_n^{(+)} \equiv \hat{A}_n^\dagger \hat{B}_n^\dagger$, $\hat{K}_n^{(-)} \equiv \hat{A}_n \hat{B}_n$, and $\hat{K}_n^{(0)} \equiv 1/2(\hat{A}_n^\dagger \hat{A}_n + \hat{B}_n^\dagger \hat{B}_n)$ that share the commutation relations $[\hat{K}_n^{(0)}, \hat{K}_n^{(\pm)}] = \pm \hat{K}_n^{(\pm)}$ and $[\hat{K}_n^{(-)}, \hat{K}_n^{(+)}] = \hat{K}_n^{(0)}$ of an $\mathfrak{su}(1,1)$ Lie algebra, which allows us to apply a specific exponential operator disentangling formula ([25], A5.18) from which the desired property is readily derived.

[18] L. Mandel and E. Wolf, *Optical Coherence and Quantum Optics* (Cambridge University Press, Cambridge, England, 1995).

[19] A. B. U'Ren, K. Banaszek, and I. A. Walmsley, Quantum Inf. Comput. **3**, 480 (2003).

[20] M. Avenhaus, M. V. Chekhova, L. A. Krivitsky, G. Leuchs, and C. Silberhorn, e-print arXiv:0810.0998.

[21] G. H. Golub and C. F. V. Loan, *Matrix Computations*, 2nd ed. (John Hopkins Press, Baltimore, MD, 1989).

[22] If $\chi^{(2)}$ were known precisely, the optimization would not be necessary.

[23] W. Mauerer, Ph.D. thesis, Max Planck Institute for the Science of Light (unpublished).

[24] G. Doetsch, Math. Z. **32**, 587 (1930).

[25] S. M. Barnett and P. M. Radmore, *Methods in Theoretical Quantum Optics* (Clarendon Press, Oxford, 1997).